Available online at www.sciencedirect.com
SCIENCE DIRECT®
International Journal of Pharmaceutics 255 (2003) 139–151
international journal of pharmaceutics
www.elsevier.com/locate/ijpharm

Insulin containing polyethylenimine–dextran sulfate nanoparticles

Waree Tiyaboonchai [a], James Woiszwillo [b], Robert C. Sims [c], C. Russell Middaugh [a,*]

[a] *Department of Pharmaceutical Chemistry, School of Pharmacy, The University of Kansas, 2095 Constant Ave., Lawrence, KS 66047-3729, USA*
[b] *Sedum Laboratories, Inc., 51 Francis Ave., Mansfield, MA 02048, USA*
[c] *Midwest Research Institute, 425 Volker Boulevard, Kansas City, MO 64110, USA*

Received 4 September 2002; received in revised form 16 January 2003; accepted 16 January 2003

Abstract

An aqueous nanoparticle delivery system has been developed which employs the oppositely charged polymers polyethylenimine (PEI) and dextran sulfate (DS) with zinc as a stabilizer. It is found that the pH of PEI solutions, the weight ratio of the two polymers, and zinc sulfate concentrations all play significant roles in controlling particle size. Spherical particles of 250 nm mean diameter were produced under optimal conditions which have a zeta potential of approximately +30 mV. Up to 90% drug entrapment efficiency was observed when insulin was used as a model protein drug. No degradation products were detected during in vitro dissolution or in potency studies. Circular dichroism (CD) spectra showed no significant conformational changes compared to free insulin under optimized formulation conditions. Rapid release characteristics were observed in in vitro dissolution studies. Biological activity in steptozotocin-induced diabetic rats, however, exhibited a prolonged hypoglycemic effect. This system offers the following advantages: (1) ease of manufacturing under mild preparation conditions; (2) employment of completely aqueous processing conditions; (3) use of biocompatible polymers which can be prepared aseptically; (4) ability to control particle size; (5) a high level of drug entrapment and (6) an ability to preserve protein secondary structure and biological activity.

Keywords: Nanoparticles; Insulin; Polyethylenimine; Dextran sulfate; Phase separation

1. Introduction

Proteins are often marginally stable and consequently easily damaged during their formulation as drugs. Nanoparticle delivery systems have been developed which have the potential to improve protein stability, increase the duration of the therapeutic effect of proteins as well as permit administration through non-parenteral routes (Florence, 1997; Gautier et al., 1992; Kreuter, 1988; Muller, 1991; Tobio et al., 1998; Zhang et al., 2001).

There are a wide variety of techniques available for producing nanoparticles including solvent evaporation, interfacial polymerization and emulsion polymerization methods. Most of these approaches, however, involve the use of organic solvents, heat or vigorous agitation, procedures which are potentially harmful to the structure and consequently biological activity of proteins (Guerrero et al., 1988; Kreuter, 1988). In this study, we describe nanoparticles that can be formed

* Corresponding author. Tel.: +1-785-864-5813; fax: +1-785-864-5814.
E-mail address: middaugh@ku.edu (C.R. Middaugh).

0378-5173/03/$ – see front matter
doi:10.1016/S0378-5173(03)00055-3

under mild processing conditions. These particles employ the oppositely charged polymers polyethylenimine (PEI) and dextran sulfate (DS) under aqueous conditions and are stabilized by crosslinking with zinc. PEI is a linear or branched chain polymer containing primary, secondary and/or tertiary amines. It has been shown to be an efficient versatile agent for in vivo gene delivery via a number of routes (Lemkine and Demeneix, 2001). PEI is often described as a "proton sponge" since its charge density is dramatically pH-dependent (Suh et al., 1994). DS is a biodegradable and biocompatible anionic polymer that has been widely used in pharmaceutical formulations. It is a branched chain polysaccharide of anhydroglucose units containing approximately 2.3 sulfate groups per glucosyl unit. The oppositely charged polymers PEI and DS self-assemble through phase separation to form nanoparticles at room temperature (Tiyaboonchai et al., 2001). While vigorous stirring or homogenization is often required during nanoparticle production, stirrer speeds of only 200–1000 rpm are necessary to form PEI/DS particles. Furthermore, heat and organic solvents are not required and particles can be easily lyophilized (Tiyaboonchai et al., 2001). Thus, this technique is in principle applicable to a broad range of labile drugs and bioactive macromolecules including proteins. This technique has so far, however, only been applied to low molecular weight small molecule drugs (Tiyaboonchai et al., 2001).

In this study, the possibility of incorporating a protein into this nanoparticle system while maintaining the protein's conformation and stability is explored. Insulin was chosen as a model protein drug since its structure, stability, and physicochemical characteristics have been extensively studied and because of its wide therapeutic utility (Brange and Langkjaer, 1993). Like many proteins, insulin tends to be destabilized by both physical and chemical stress and its biological activity subsequently easily altered (Sluzky et al., 1991).

2. Materials and methods

2.1. Materials

Bovine insulin (MW 5733), polyethylenimine (MW 50,000), dextran sulfate (MW 500,000), mannitol, zinc sulfate, and steptozotocin (STZ) were obtained from Sigma, St. Louis, MO, USA. All other chemicals and solvents were of analytical grade. Cellulose ester dialysis membrane tubing with a molecular weight cut-off (MWCO) of 1,000,000 (Spectra/Por CE) and regenerated cellulose dialysis membrane tubing with a MWCO of 15,000 (Spectra/Por RC), both with diameters of 15 mm, were purchased from Fisher Scientific (Chicago, IL, USA). Male Sprague–Dawley rats were purchased from Charles River Laboratories (Indianapolis, IN, USA).

2.2. Methods

2.2.1. Preparation of empty and insulin-loaded PEI–DS nanoparticles

Nanoparticles were prepared at room temperature. One hundred microliters of insulin solution (0.7 mg/ml) in 0.01N HCl, 0.2 ml of 1% (w/v) DS solution, and 0.3 ml of aqueous PEI solution (1%, w/v) were mixed with 10 mM tris buffer, pH 8, in a final volume of 1 ml at 500 rpm for 2 min. Twenty five microliters of 1 M zinc sulfate solution was added and the resulting nanoparticles were stirred for 5 min. The stabilized insulin nanoparticles were washed for 24 h in the dark by dialysis against a 5% (w/v) mannitol solution using Spectra/Por CE with a MWCO of 1,000,000. This dialysis medium was chosen based on results from previous work (Tiyaboonchai et al., 2001) which showed no alteration of the mean particle size under such conditions. The purified, loaded nanoparticles were frozen and lyophilized (Virtis freezemobile 5SL, Gardiner, NY, USA) at 1272 mTorr and −46 °C for 24 h. Lyophilized nanoparticles were stored in a desiccator at 2–8 °C. Samples were prepared in duplicate.

Process parameters were varied as follows: the pH of a 1% (w/v) PEI solution was varied from 7 to 10 and adjusted by the addition of a 1.0N HCl solution; the concentration of zinc sulfate was varied from 0 to 35 μM and the PEI to DS weight ratio from 0.5:1 to 3:1. Empty nanoparticles were prepared using the same procedures.

2.2.2. Physicochemical characterization of the nanoparticles

The morphology of both unloaded and insulin-loaded particles was investigated using transmission electron microscopy (TEM, JEM-1200EXII, JEOL, Japan) following negative staining with sodium

phosphotungstate solution (2%, w/v). An aliquot of lyophilized nanoparticles was resuspended in 1 ml of nanopure water and then dialyzed against the same solution for 24 h (using dialysis tubing MWCO 15,000) to remove mannitol from the sample. Five microliters of both the sample and a 2% (w/v) phosphotungstate solution were placed on a 300 mesh copper grid with a carbon-coated Formvar membrane. Excess solvent was removed using Whatman no. 1 filter paper and the sample was stored in a desiccator overnight before examination by TEM. Scanning electron microscopy (SEM, S-570, Hitachi, Japan) was used to examine the surface and shape of particles. The lyophilized particles were sprinkled onto a conductive tab on a stud and sputter coated with 20 nm gold–palladium (60:40) in a cathode evaporator prior to analysis.

The mean particle size of nanoparticles before and after lyophilyzation was determined by dynamic light scattering (DLS) employing a Brookhaven system (Holtsville, NY, USA). This instrument was fitted with a 50 mW HeNe diode laser operating at 532 nm (JDS Uniphase, San Jose, CA, USA), and a BI-200SM Goniometer with an EMI 9863 photomultiplier tube connected to a BI-9000AT digital correlator card. An aliquot of lyophilized particles was resuspended in nanopure water. Measurements were then performed at 90° to the incident light and data was collected over a period of 3 min. The mean particle size and polydispersity were obtained by the method of cumulants (Koppel, 1972).

The zeta potential of nanoparticles was determined using phase analysis light scattering employing a ZetaPALS instrument (Brookhaven Instruments Corporation, Holtsville, NY, USA). The instrument was equipped with a 25 mW solid state laser operating at 676 nm. The measurement angle was 15° to the incident beam. Samples were prepared by redispersing 4 mg of lyophilized particles in 1.3 ml of water. Data was then collected for 10 cycles and a minimum of three measurements were performed on each sample. The zeta potential was calculated from the electrophoretic mobility using the Smoluchowski approximation.

2.2.3. Determination of entrapment efficiency

Twelve milligrams of lyophilized nanoparticles prepared as described above were weighed and dissolved in 0.5 ml of 0.05N HCl. This solution was centrifuged at 12,000 × *g* for 20 min. Five samples were analyzed under each set of conditions examined. The amount of associated insulin was directly determined from the second derivative of the insulin absorption band at 277 nm employing a calibration curve from 0.1 to 0.5 mg/ml of insulin in 0.05N HCl. The percent drug association was then calculated from the following equation:

$$\%\ \text{drug association} = \frac{\text{amount of insulin in particle} \times \text{volume tested}}{\text{total sample volume} \times \text{initial amount of insulin}} \times 100\% \quad (1)$$

where the amount of insulin refers to weight quantities of the protein.

2.2.4. Potency and purity of insulin in nanoparticles

The potency of insulin-loaded lyophilized nanoparticles was examined by an HPLC method modified from Hoyer et al. (1995). An HPLC apparatus (SCL-6B, Shimadzu, Columbia, MD, USA) equipped with a UV-Vis detector (SPD-6AV, Shimadzu) was used. The column (250 mm × 4.6 mm i.d.) was packed with a matrix of octadecylsilane-coated 5 μm silica beads of 300 Å pore size (Vydac C4, The Separations Group, Hesperia, CA, USA). The mobile phase was composed of 50 mM phosphate buffer, pH 2.4, and acetonitrile (73:27). A flow rate of 1.0 ml/min and a detection wavelength of 230 nm were employed. 200 μg/ml of standard insulin was prepared in 0.01N HCl. Nanoparticles containing 200 μg of insulin were dissolved in 1.0 ml of 0.05N HCl. The solution was centrifuged at 12,000 × *g* for 20 min before injection onto the column. The potency of insulin was calculated from the following relationship: Cu = Cs × Ru/Rs where Cu: potency of unknown, Cs: potency of standard, Ru: peak area of unknown and Rs: peak area of standard.

2.2.5. Circular dichroism spectroscopy

Circular dichroism (CD) spectra were obtained with a Jasco J-720 spectropolarimeter (Hachioji city, Tokyo, Japan) equipped with a pelltier temperature controller. Spectra were collected at 20° C using a 0.1 cm cell over the wavelength range of 190–270 nm. A resolution of 0.1 nm and scanning speed of 10 nm/min with a 2 s response time were

employed. Each spectrum obtained represents an average of three consecutive scans in molar ellipticity units (θ_m, deg M^{-1} cm^{-1}). Noise reduction, blank buffer subtraction, and data analysis were performed using Standard Analysis and Temperature/Wavelength Analysis programs (Jasco). Secondary structure content was estimated employing CDPro software with data in the range of 190–240 nm using the basis 4 and 7 program for input data (Sreerama et al., 1999). The results represent an average of values obtained from SELCON3, CONTINLL and CDsstr programs. Loaded nanoparticles suspensions containing 0.1 mg/ml of insulin were dialyzed against water at 4 °C in a dark room for 24 h before analysis by CD. Standard insulin solutions were prepared at 0.1 mg/ml in 10 mM phosphate buffer, pH 7.0.

2.2.6. In vitro dissolution studies

In vitro release of insulin nanoparticles was studied at 37 ± 0.5 °C in 5 and 10 mM phosphate buffer and 50 mM phosphate buffer containing 0.15 M NaCl, all at pH 7.4. Albumin (0.2%, w/v) was added to the dissolution medium to counteract non-specific adsorption of insulin to the glass surface. Nanoparticles containing 15 μg of insulin were placed into 20 ml of the dissolution medium and stirred at 200 rpm in the dark. Aliquots (1 ml) were taken at predetermined time intervals. Samples were filtered through a 0.2 μm membrane and the amount of insulin released was determined using the HPLC method described above for the potency studies with a detection wavelength of 214 nm. Dissolution studies were performed in triplicate. Insulin content was determined by peak area using a linear calibration curve constructed from 5 to 20 μg/ml of standard insulin solution.

2.2.7. Biological activity in steptozotocin-induced diabetic rats

Male Sprague–Dawley rats were fasted for 12–16 h prior to inducing diabetes melitus. 60 mg/ml of STZ in acetate buffer, pH 4.5, was freshly prepared and used within 1 h. Prior to injection, approximately 300 μl of blood was collected by the retro-orbitary sinus method to determine baseline serum glucose levels. Each rat was injected with a single intraperitoneal (i.p.) dose of STZ solution at 60 mg/kg 5 days prior to study. Fasted rats with blood glucose level >250 mg/dl were considered diabetic. Prior to administration of insulin, STZ-induced diabetic rats were fasted for 12–16 h. Insulin (0.35 IU/kg) in PBS, insulin nanoparticles (equivalent to 0.35 IU/kg insulin) in phosphate buffer or sterile water were injected subcutaneously into the diabetic rats. The variability of the mean size and potency of these particles was less than 5%. Blood samples were collected from the retro-orbitary sinus at predetermined time points of 0, 1, 2 and 4 h. Blood samples were left at room temperature for clotting and then centrifuged (∼3500 rpm, 2–8 °C, ∼10 min) to obtain serum for analysis. Serum samples were stored at approximately −20 °C prior to glucose analysis. Serum glucose levels were measured with a COBAS Mira chemistry analyzer (Roche, Branchburg, New Jersey, USA) using a standard hexokinase/glucose-6-phosphate dehydrogenase assay (Roche, Branchburg, New Jersey).

3. Results

3.1. Morphology

The structure of insulin-loaded and unloaded lyophilized nanoparticles was examined by SEM and TEM. SEM micrographs of empty and insulin-loaded nanoparticles show that the particles have a uniform spherical shape and a smooth surface (Fig. 1A and B). TEM images of insulin-loaded and unloaded nanoparticles also display spherical particles (Fig. 2A and B). The darker edge seen around many particles may represent the wall of the nanoparticles or excess PEI coated on the particle surface. Both SEM and TEM micrographs also illustrate that some particles are agglomerated while others are uniformly distributed as single particles. Variation in processing parameters (see below) had no effect on the appearance of the particles.

3.2. Size and zeta potential

The effect of processing conditions on the mean particle size and polydispersity of insulin nanoparticles before and after lyophilization was studied by DLS. All formulations (Table 1) were initially examined at a polymer ratio of 1.5:1 with 25 μM zinc sulfate and the pH of PEI solutions was varied from

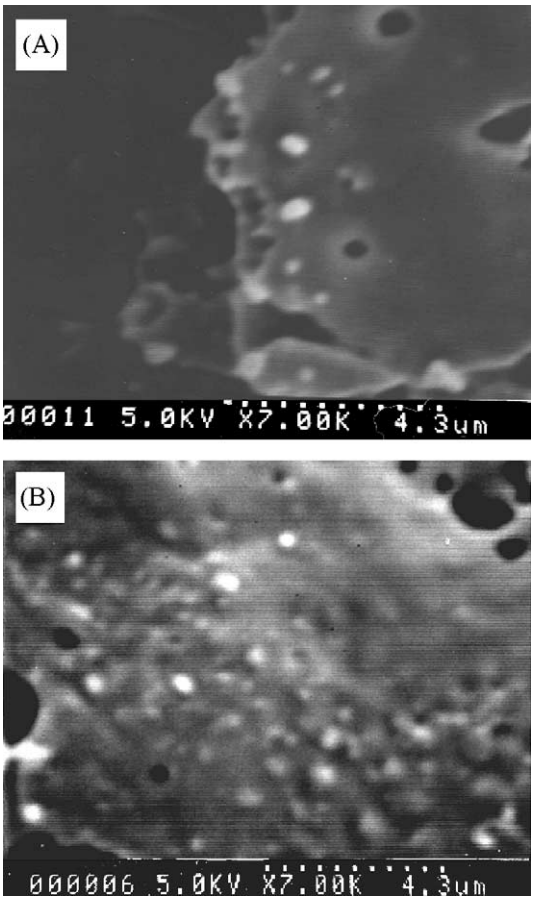

Fig. 1. SEM micrographs of nanoparticles formed using a pH 9 PEI solution and a PEI:DS mass ratio of 2.5:1. The particles were washed in 5% (w/v) mannitol. (A) Unloaded nanoparticles and (B) insulin-loaded nanoparticles.

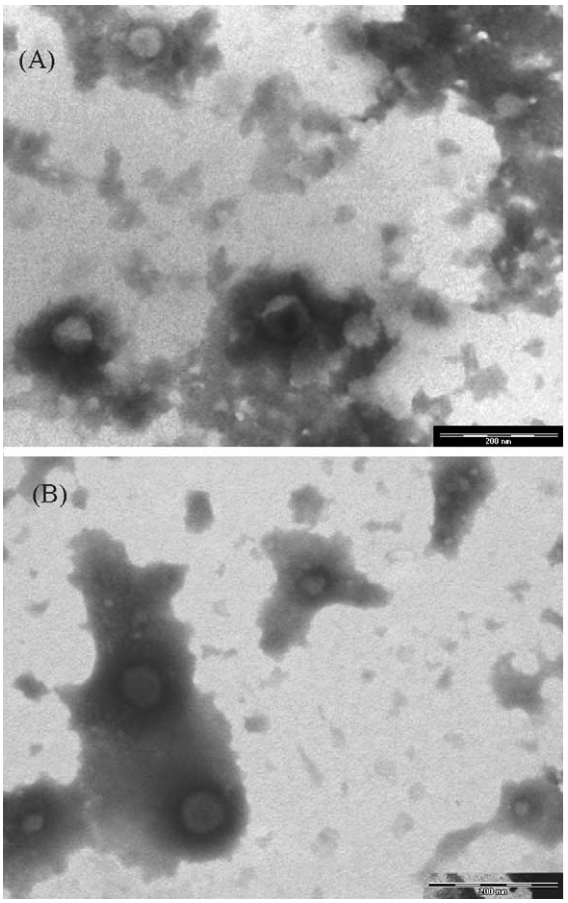

Fig. 2. TEM micrographs of nanoparticles formed employing a pH 9 PEI solution and a PEI:DS mass ratio of 2.5:1. (A) Unloaded nanoparticles and (B) insulin-loaded nanoparticles. The scale bar represents 200 nm in length.

7 to 10. It should be noted that in free solution between pH 4 and 8, insulin associates into a hexamer in the presence of zinc even at low protein concentrations (>0.01 mM). Precipitation was observed at pH 7 and 8, while narrow size distributions and 360 and 190 nm particles were obtained with PEI solutions at pH 9 and 10, respectively. The effect of the ratio of PEI to DS (varied from 0.5:1 to 3:1) on particle size

Table 1
Effect of PEI solution pH on mean particle size, polydispersity, and zeta potential of insulin-loaded nanoparticles

pH of PEI solution	Before lyophilization	After lyophilization		Zeta potential (mV)
	Mean (nm) ± S.D.	Mean (nm) ± S.D.	Polydispersity index	
7	NM	–	–	–
8	NM	–	–	–
9	308 ± 27	364 ± 10	0.17	+26
10	354 ± 18	191 ± 21	0.26	+27

NM: micron size particles which could not be measured by DLS; preparation conditions: PEI:DS ratio of 1.5:1; 25 μM zinc sulfate.

Table 2
Effect of polymer ratios on mean particle size, polydispersity, and zeta potential of insulin-loaded nanoparticles

Polymer ratio (PEI:DS)	Before lyophilization	After lyophilization		Zeta potential (mV)
	Mean (nm) ± S.D.	Mean (nm) ± S.D.	Polydispersity index	
0.5	NM	–	–	–
1	NM	–	–	–
1.5	308 ± 27	364 ± 10	0.17	+26
2	269 ± 18	309 ± 8	0.16	+27
2.5	246 ± 11	277 ± 5	0.16	+28
3	230 ± 15	236 ± 14	0.19	+26

NM: micron size particles which could not be measured by DLS; preparation conditions: pH 9 PEI solution; 25 μM zinc sulfate.

was investigated by maintaining the amount of zinc sulfate at 25 μM and employing PEI solutions at pH 9. The results show that as this ratio is increased, the mean particle size decreases (Table 2). The effect of zinc sulfate concentration on the mean particle size was also studied. When formulated at a PEI:DS ratio of 1.5:1 (pH 9 PEI solutions), it was found that 15–25 μM zinc sulfate was optimal in producing stable nanoparticles (Table 3). At higher concentrations of zinc sulfate (35 μM), precipitation was observed. Preparations formulated without zinc sulfate showed a mean particle size twice that before lyophilization. In the presence of zinc sulfate, however, particle size remained constant before and after lyophilization. Overall, as the amount of zinc sulfate was increased, the particle size decreased. These results suggest that zinc sulfate may stabilize the nanoparticles through electrostatic interactions with the nanoparticles.

Zeta potential studies of nanoparticles show that there are no significant differences in zeta potential (+26 mV) when the pH of PEI solutions is varied or the polymer ratio is modified (Tables 1 and 2). The zeta potential of nanoparticles, however, increases with decreasing amounts of zinc sulfate (Table 3). Particles in the presence or absence of 5 μM zinc sulfate possessed a zeta potential of +60 mV. The zeta potential of unloaded nanoparticles showed the same trend when zinc sulfate concentration was altered (not illustrated). Suspensions of particles in the absence of zinc possessed a pH of 9.5, whereas particles in the presence of 25 μM zinc sulfate produced a solution pH of 6.8. Particles in the absence of zinc would thus appear to have more unprotonated amine groups available on their surfaces than those formulated with zinc. When these particles (pH 9.5) were dialyzed against a pH 7 mannitol solution, free amines on the surfaces of zinc-free particles presumably became more protonated than those in formulations containing more than 5 μM zinc sulfate. This difference in protonation state is then reflected in higher zeta potential values.

3.3. Entrapment efficiency

The association of insulin with the particles appears to be an efficient process. Most of the formulations studied demonstrated an entrapment efficiency of 80–90%. For example, the formulations described in Table 2 demonstrated entrapment efficiencies of

Table 3
Effect of zinc sulfate concentration on mean particle size, polydispersity, and zeta potential of insulin-loaded nanoparticles

[$ZnSO_4$] (μM)	Before lyophilization	After lyophilization		Zeta potential (mV)
	Mean (nm) ± S.D.	Mean (nm) ± S.D.	Polydispersity index	
0	384 ± 61	676 ± 46	0.27	+65
5	350 ± 26	536 ± 45	0.32	+62
15	344 ± 27	345 ± 25	0.25	+27
25	308 ± 27	364 ± 10	0.17	+26
35	NM	–	–	–

NM: micron size particles which could not be measured by DLS; preparation conditions: pH 9 PEI solution; PEI:DS ratio of 1.5:1.

83.3 ± 2.1–89.9 ± 2.7% as the polymer ratio was varied from 0.5 to 3 after lyophilization. Processing conditions also did not have a significant impact on the extent of drug association.

3.4. Stability and potency of insulin in nanoparticles

Reverse phase HPLC chromatograms of insulin-loaded particles dissolved in 0.05N HCl manifest the same retention time and peak shape as those of standard insulin. Furthermore, no additional peaks were observed. The potency of standard insulin is 28.5 U/mg. The potency of insulin extracted from the nanoparticles was in the range of 27–28 U/mg or 95–99% that of free insulin. The main peak of insulin was about 99% of the total peak area for both standard and released insulin. Thus, there appear to be no detectable differences in potency or purity of the insulin in the nanoparticles preparations compared to standard insulin. These results suggest that there was no significant insulin degradation upon incorporating insulin into PEI–DS particles. In addition, after storage in a desiccator at 2–8 °C for 6 months, insulin associated with nanoparticles manifested the same potency and purity as the initial preparation (not illustrated).

3.5. The secondary structure of insulin within nanoparticles

The CD spectrum of 0.1 mg/ml insulin in 5 mM phosphate buffer, pH 7, shows a maxima at 196 and minima at 209 and 222 nm (Fig. 3). The estimated secondary structural content of insulin was 41% α-helix, 17% β-sheet, and 41% irregular (Table 4). The CD spectrum and secondary structure content of insulin were in close agreement with results presented by other investigators (e.g. Pocker and Biswas, 1980). The effect of PEI solution pH on the conformation

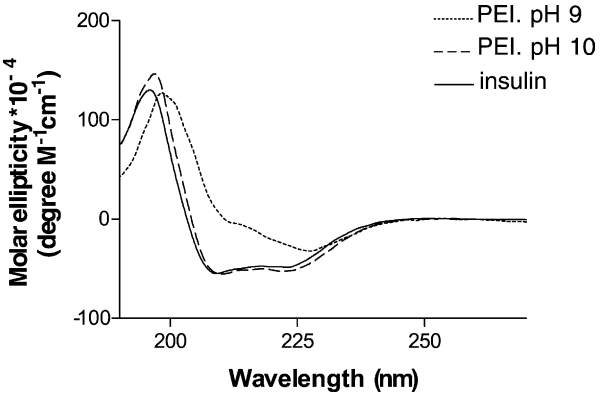

Fig. 3. CD spectra of (—) free insulin and insulin within particles formulated at a PEI:DS ratio of 1.5:1, 25 μM zinc sulfate, using PEI solutions at: (···) pH 9 and (- - -) pH 10.

of particle associated insulin was investigated using formulations with a PEI:DS ratio of 1.5:1 and 25 μM zinc sulfate. The CD spectrum of loaded particles formulated at pH 10 was not significantly different than that of standard insulin, while particles formulated at pH 9 produced a red-shifted spectrum of reduced intensity (Fig. 3). The spectrum of insulin particles formulated at pH 9 suggests that under these conditions the protein possesses more β-sheet and less α-helix character than free insulin (Table 4). At this pH, however, the CD spectra of formulations containing other polymer ratios indicate that insulin conformation is better preserved at PEI:DS ratios of ≥2:1 (Table 5). At these higher polymer ratios, the CD spectra did show some small red shifts and slightly lower intensities at 209 nm compared to standard insulin (Fig. 4).

The effect of zinc sulfate concentration on insulin secondary structure formulated with pH 9 PEI solutions at a PEI:DS ratio of 1.5:1 was also marked. CD spectra of insulin-loaded particles show decreasing intensities at 209 and 223 nm with increasing amounts of zinc sulfate (Fig. 5). These changes correspond to

Table 4
Effect of PEI solution pH on the conformation of insulin within nanoparticles compared to the conformation of free insulin solution, pH 7

pH of PEI solutions	α-Helix (% ± S.E.M.)	β-Strand (% ± S.E.M.)	Turn (% ± S.E.M.)	Unordered (% ± S.E.M.)
Insulin	41 ± 1	17 ± 2	13 ± 2	28 ± 4
9	17 ± 7	35 ± 3	19 ± 6	29 ± 5
10	49 ± 3	16 ± 4	9 ± 6	25 ± 7

Preparation conditions: PEI:DS ratio of 1.5:1; 25 μM zinc sulfate; S.E.M.: standard error of mean.

Table 5
Effect of polymer ratios on the conformation of insulin within nanoparticles compared to the conformation of free insulin solution, pH 7

Polymer ratios (PEI:DS)	α-Helix (% ± S.E.M.)	β-Strand (% ± S.E.M.)	Turn (% ± S.E.M.)	Unordered (% ± S.E.M.)
Insulin	41 ± 1	17 ± 1	13 ± 1	28 ± 3
1.5	17 ± 7	35 ± 3	19 ± 6	29 ± 5
2.0	37 ± 7	23 ± 6	13 ± 9	28 ± 10
2.5	40 ± 5	21 ± 4	14 ± 5	25 ± 5
3	42 ± 5	19 ± 4	13 ± 5	27 ± 6

Preparation conditions: pH 9 PEI solution; 25 μM zinc sulfate; S.E.M.: standard error of mean.

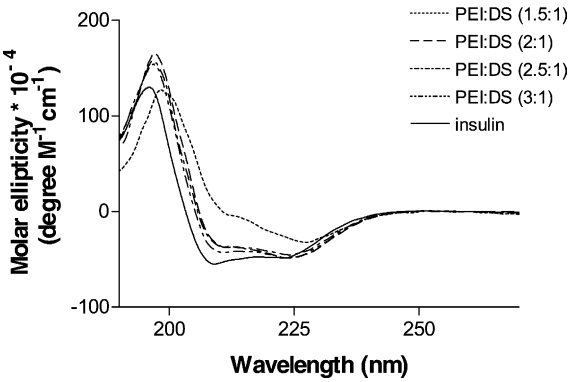

Fig. 4. CD spectra of (—) free insulin and insulin within nanoparticles formulated with pH 9 PEI solution using 25 μM zinc sulfate at various PEI:DS ratios; (···) 1.5:1; (---) 2:1; (-·-) 2.5:1; and (-···) 3:1.

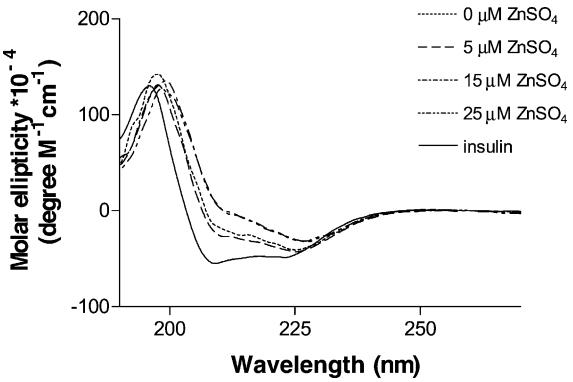

Fig. 5. CD spectra of (—) free insulin and insulin particles formulated at a PEI:DS ratio of 1.5:1 using pH 9 PEI solutions containing various amounts of zinc sulfate; (···) 0 μM; (---) 5 μM; (-·-) 15 μM; and (-···) 25 μM.

a structural change from α-helix to β-sheet (Table 6). Thus, these results suggest that at the lower polymer ratio (1.5:1), the presence of zinc enhances insulin β-sheet content. At higher polymer ratios (≥2:1), however, zinc had no significant impact on the secondary structure of entrapped insulin (Tables 5 and 6).

The intensity of the molar ellipticity of free insulin at 222 nm gradually decreased as the temperature was increased from 25 to 85 °C (Fig. 6A). A small change in intensity at 209 was also observed. The ratio of the molar ellipticity at 209 and 222 nm gradually increased from a value of 1.2 at 10 °C to a value of 2 with increasing temperature. These observations suggest that the quaternary conformation of insulin changes from that of hexamer to dimer and monomer as the temperature increased (Pocker and Biswas, 1980). In contrast, melting curves of insulin in PEI–DS particles formulated at pH 9 and 10 show more cooperative transitions

Table 6
Effect of zinc sulfate concentration on the conformation of insulin within nanoparticles compared to the conformation of free insulin solution, pH 7

Zinc sulfate (μM)	α-Helix (% ± S.E.M.)	β-Strand (% ± S.E.M.)	Turn (% ± S.E.M.)	Unordered (% ± S.E.M.)
Insulin	41 ± 2	17 ± 2	13 ± 2	28 ± 4
0	24 ± 4	31 ± 4	18 ± 5	27 ± 7
5	25 ± 4	29 ± 4	18 ± 55	28 ± 4
15	14 ± 6	37 ± 5	18 ± 7	30 ± 6
25	17 ± 7	35 ± 3	19 ± 6	29 ± 5

Preparation conditions: pH 9 PEI solution; PEI:DS ratio of 1.5:1; S.E.M.: standard error of mean.

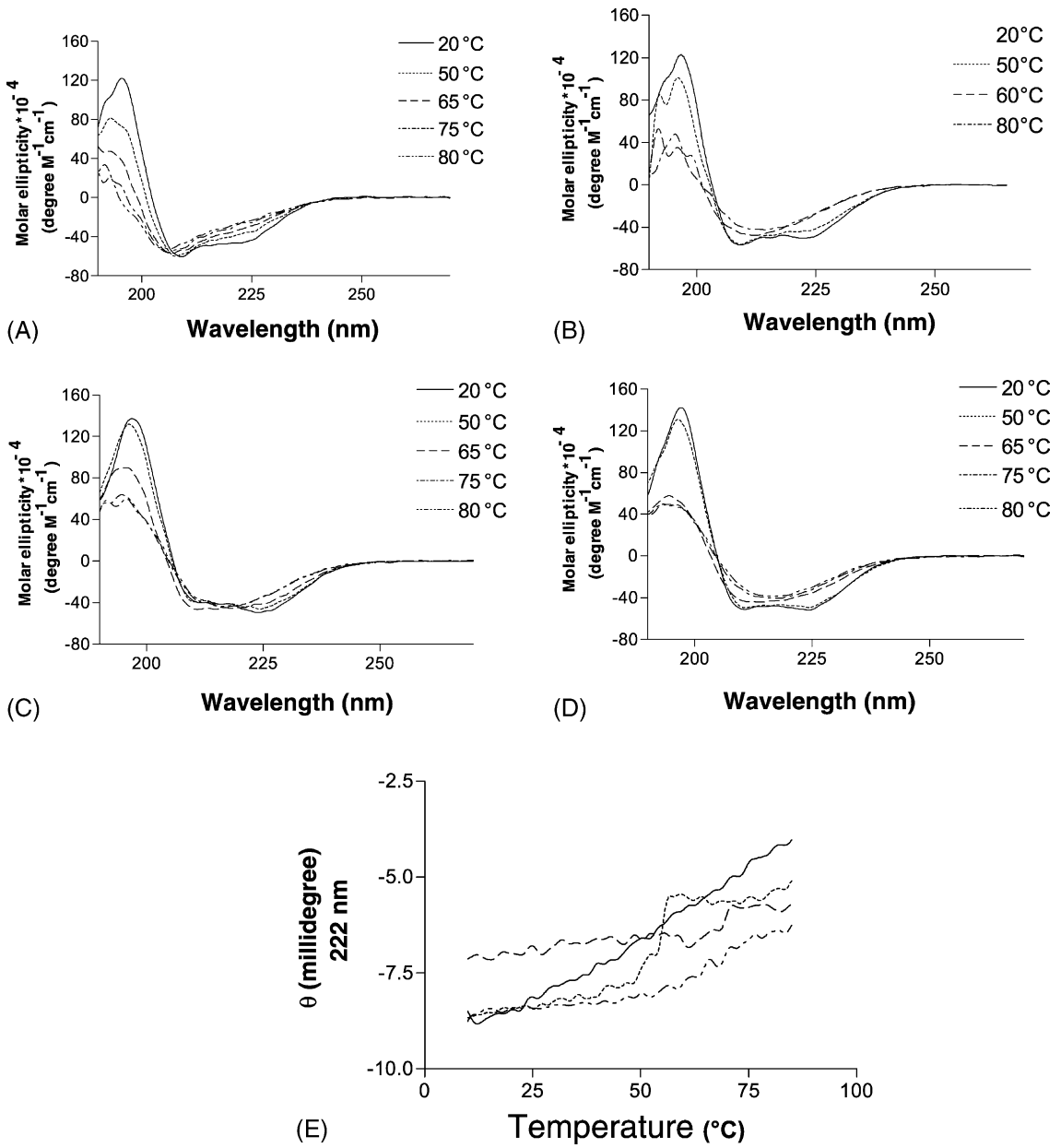

Fig. 6. CD spectra of free insulin and insulin complexes at different temperatures are shown in panels A–D; (panel A) free insulin; (panel B) insulin–PEI complexes in the absence of DS; (panel C) insulin–PEI–DS nanoparticles formulated at pH 9 PEI solution with PEI:DS ratio of 2.5:1; (panel D) insulin–PEI–DS nanoparticles formulated at pH 10 PEI solutions with PEI:DS ratio of 1.5:1. Effect of temperature on the ellipticity of free insulin and insulin complexes at 222 nm are shown in panel E: (—) free insulin; (···) insulin–PEI complex in the absence of DS; (- - -) insulin nanoparticles formulated at pH 9 PEI solution with PEI:DS ratio of 2.5:1; and (-···-) insulin nanoparticles formulated at pH 10 PEI solutions with PEI:DS ratio of 1.5:1.

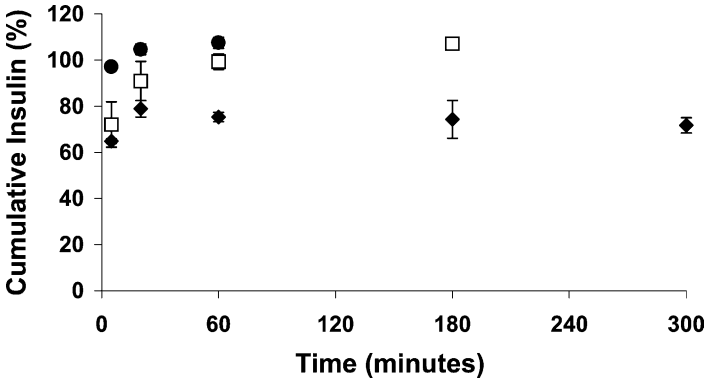

Fig. 7. In vitro release of insulin loaded particles prepared with a pH 9 PEI solution with a PEI:DS ratio of 2:1 in different dissolution media: (●) 50 mM PBS, pH 7.4; (□) 10 mM phosphate buffer, pH 7.4; and (◆) 5 mM phosphate buffer, pH 7.4.

at 70 and 55 °C, respectively (Fig. 6E). Insulin–PEI complexes (no DS) produce a transition at 40 °C (Fig. 6E). Unlike free insulin, however, substantial changes in double minima at 209 and 222 nm to a single negative peak at 215 nm are observed in both complexes (Fig. 6B and D). This suggests some α-helix to β-sheet transition in these particles at elevated temperatures and that PEI may facilitate insulin fibrillation.

3.6. In vitro dissolution studies

The time-dependent cumulative percent release of insulin from nanoparticles in 50 mM PBS was examined. In most formulations, insulin was completely released from nanoparticles within 5 min, independent of PEI solution pH and polymer ratio (Fig. 7). Zinc-free nanoparticles, however, released only 70%

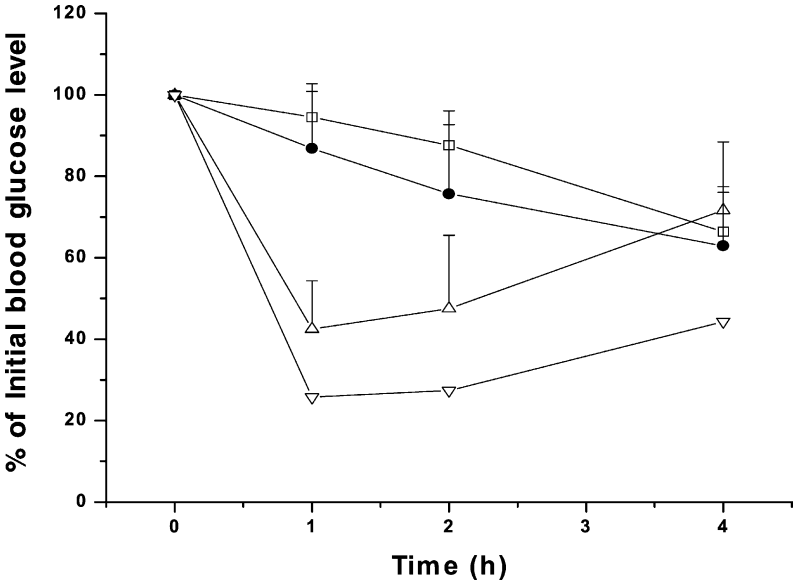

Fig. 8. Effect of insulin and insulin nanoparticles injected subcutaneously (all at equivalent insulin dose levels of 0.35 IU/kg) to SZT-induced diabetic rats on the reduction of blood glucose level: (▽) free insulin; insulin particles formulated with zinc sulfate with (●) a PEI:DS ratio of 2.5:1; (□) a PEI:DS ratio of 1.5:1; and (△) insulin particles formulated in the absence of zinc sulfate with a pH 9 PEI solution at a PEI:DS ratio of 1.5:1. Each point represents the mean ± S.E.M. of 3–4 rats. Only two diabetic rats were subcutaneously injected with the free insulin solution.

of the insulin within 5 min whereas 75% of the insulin was released at 7 h. After 7 h, the amount of insulin detected in the dissolution medium continued to decrease which may reflect some insulin degradation.

The drug release profile in lower ionic strength media was also investigated. In 10 mM phosphate buffer, insulin is released rapidly and completely with a 70% burst release at 2 h. In contrast, only 70% of the insulin was released within 6 h following a 65% burst release in 5 mM phosphate buffer. The effect of ionic strength on insulin release kinetics suggests that the protein interacts with PEI–DS nanoparticles at least partially through electrostatic interactions. HPLC chromatograms of insulin released from particles over these time intervals show the same peak shape and retention time as standard insulin. An absence of additional peaks indicates that no degradation products are formed during the early release process.

3.7. In vivo biological activity

After the subcutaneous injection of free insulin (0.35 IU/kg) into fasted induced diabetic rats, approximately 20% of the initial blood glucose levels (BGL) were reached within 1–2 h (indicating a hypoglycemic effect) (Fig. 8). Blood glucose levels, however, started to increase 2 h after administration of free insulin suggesting as expected, a rapid onset and relatively short duration of action of free insulin. The same trend in temporal glucose levels was seen with insulin nanoparticles formulated in the absence of zinc sulfate at a PEI:DS ratio of 1.5:1 suggesting a similar short duration of action as well. In contrast, insulin–PEI–DS nanoparticles in the presence of zinc produced a gradual decrease in BGL over 4 h indicating a more sustained effect. For ethical reasons, food was return to the animal after the 4-h time point and only data collected during fasting period was evaluated. Nevertheless, a downward trend in the zinc-stabilized insulin nanoparticles is apparent.

4. Discussion

We find that insulin can be incorporated into PEI–DS nanoparticles with high efficiency. In previous work, a small insoluble molecule (amphotericin B) was incorporated into similar PEI–DS nanoparticles employing a PEI solution at pH 8 and the effect of processing conditions on the mean particle size was extensively explored (Tiyaboonchai et al., 2001). In this study, nanoparticle precipitation was observed under suboptimal conditions. More optimal formulation conditions were found, however, that employ PEI solutions at pH 9, a PEI:DS mass ratio of $\geq$2:1, and 25 μM zinc sulfate. It was found that as the ratio of the polymers was increased, the mean particle size decreased. The finding that the optimal PEI:DS ratio for formulating insulin nanoparticles was $\geq$2:1 suggests that PEI may act as colloidal protectant, preventing particles from agglomeration through steric hindrance. Under optimal conditions, spherical particles with a mean particle size of approximately 250 nm and a polydispersity index of 0.2 (indicating a relatively narrow size distribution) were achieved. Similar results were obtained with batch sizes up to 1 l, the largest tested.

Particles were formed rapidly when PEI was added to insulin–DS solutions as evidenced by the appearance of turbidity. Insulin has an apparent pI of 6.4 (Kaarsholm et al., 1990) and a charge of −2 at a final system pH of ∼6.8. Electrostatic interactions between PEI and DS are an obvious mechanism of interaction since the polymers are oppositely charged at this pH (Tiyaboonchai et al., 2001). Circular dichroism studies of the PEI–insulin interactions in the absence of DS find that the conformation of insulin alters from primarily α-helical to one containing more β-sheet at low PEI concentrations. The structurally altered insulin, however, completely dissociates from PEI in higher (153 mM NaCl) ionic strength medium and returns to a native-like conformation as indicated by a reversal of the CD spectrum. In contrast, 70% of particle-bound insulin is dissociated from PEI–DS particles in 10 mM phosphate buffer within 5 min. The rapid release of insulin from the PEI–DS nanoparticles in hypotonic medium suggest that much of the insulin might be adsorbed on the particles' surface through apolar interactions.

Maintenance of the structural integrity of a therapeutic protein during formulation and storage is crucial for its biological efficacy. Thus, the secondary structure of insulin within nanoparticles was investigated using CD. These CD results suggest that PEI is responsible for the observed conformational changes of associated insulin since no structural perturbations

were detected in the presence of DS alone. Additionally, the CD spectra of insulin in insulin–PEI–DS nanoparticles closely resembled those of insulin–PEI complexes alone. The effect of PEI on bound insulin seems to be strongly influenced by the conformation and charge density of PEI and therefore strongly depends on the solution pH and the concentration of the polycationic component.

Insulin associated with PEI–DS particles manifested CD-detected conformational changes when formed with PEI solutions at pH 9, at a PEI:DS ratio of 1.5:1. These results can be rationalized by a nearest-neighbor interaction model (Satake and Yang, 1976). This approach considers distinct apolar interactions between amphiphiles adsorbed to a linear array of charged binding sites on a polyelectrolyte. Thus, as the pH of a PEI solution is decreased, protonation increases. This causes PEI to adopt an extended coil conformation of high charge density and shorter distance between charges. This will in turn lead to partial unfolding of the insulin molecules and then subsequent hydrophobic association. As commonly seen with proteins, this association may be mediated by intermolecular β-structure formation as suggested by the CD results. In contrast to the findings when pH 9 PEI solutions are employed at a polymer ratio of 1.5:1, the use of pH 10 PEI solutions at a PEI:DS ratio of 1.5:1, or pH 9 PEI solutions at a polymer ratio of $\geq$2:1, produce no detectable conformation changes. At higher pH values (e.g. pH 10), however, only 7% of the PEI's amine are protonated. In this situation, as well as at high concentrations of PEI, the polymers should adopt a less extended conformation of much lower charge density. This should lead to decreased structural disruption of the adsorbed insulin molecules and less self-association.

It is well establish that insulin undergoes a partial structural change from helix to sheet during fibril formation (Bouchard et al., 2000; Brange and Langkjaer, 1993; Yeo et al., 1994). These fibrils are generally biologically inactive. Activity may be recovered, however, upon dissolving the protein in alkaline medium (pH > 11, followed by neutralization) (Brange and Langkjaer, 1993). Although the conformational changes seen here appear to mimic those seen in fibril formation, the resultant structures differ in solubility properties. Insulin fibrils are insoluble in most aqueous media, including mineral acid (Brange and Langkjaer, 1993). Potency studies here, however, find that 0.05N HCl extracted insulin retains 99% of its potency. Dissolution studies in isotonic buffer (50 mM PBS, pH 7.4) also found complete insulin release with the protein possessing normal chromatographic behavior. These results argue that insulin fibrils are not formed within the PEI–DS nanoparticles. Moreover, a hypoglycemic effect in diabetic rats was produced by the nanoparticles regardless of polymer ratio indicating preservation of biological activity despite the detection of small insulin structural changes. Thus, the conformational changes of insulin that are seen suggest the presence of reversible nonfibrillar aggregates of partially unfolded insulin (Yeo et al., 1994).

Zinc sulfate probably stabilizes the particles through interactions with dextran sulfate. Thus, an effect on insulin release might be expected with increasing zinc sulfate. In vitro dissolution studies, however, found rapid release of the protein when the particles were formulated with or without zinc sulfate. These rapid release characteristics were confirmed by in vivo biological activity studies that are consistent with rapid release kinetics of insulin from nanoparticles prepared in the absence of zinc sulfate.

Additionally, zinc-free nanoparticles produced the same bioavailability as free insulin. In contrast, insulin containing zinc sulfate stabilized particles released the protein more slowly over the 4 h period examined. A possible explanation for the apparently prolonged release may be that excess zinc can diffuse into the insulin itself and form 2- and/or 4-zinc insulin species over the pH range of 4–8. Dynamic light scattering studies are consistent with this hypothesis (not illustrated). Zinc bound insulin hexamers are known to be more stable than the unliganded protein. This could result in a slow release of the monomeric (biologically active) form upon subcutaneous injection (Hallas-Moller, 1956; Smith et al., 1984).

Acknowledgements

Waree Tiyaboonchai would like to thank the Royal Thai Government for financial support.

References

Bouchard, M., Zordo, J., Nettleton, E.J., Dobson, C.M., Robinson, C.V., 2000. Formation of insulin amyloid fibrils followed by FTIR simultaneously with CD and electron microscopy. Protein Sci. 9, 1960–1967.

Brange, J., Langkjaer, L., 1993. Insulin structure and stability. In: Wang, Y.J., Pearlman, R. (Eds.), Stability and Characterization of Protein and Peptide Drugs. Plenum Press, New York, pp. 315–350.

Florence, A.T., 1997. The oral absorption of micro- and nanoparticulates: neither exceptional nor unusual. Pharm. Res. 14, 259–266.

Gautier, J.C., Grangier, J.L., Barbier, A., DuPont, P., Dussossory, D., Pastor, G., Couvreur, P., 1992. Biodegradable nanoparticles for subcutaneous administration of growth hormone releasing factor (hGRF). J. Control. Release 20, 67–78.

Guerrero, D.Q., Allemann, E., Fessi, H., Doelker, E., 1988. Preparation techniques and mechanisms of formation of biodegradable nanoparticles from performed polymers. Drug Dev. Ind. Pharm. 24, 1113–1128.

Hallas-Moller, K., 1956. The 'Lente' insulins. Diabetes 5, 7–14.

Hoyer, G.L., Nolan, P.E.J., LeDoux, J.H., Moore, L.A., 1995. Selective stability-indicating high-performance liquid chromatographic assay for recombinant human regular insulin. J. Chromatogr. 699, 383–388.

Kaarsholm, N.C., Havelund, S., Hougaard, P., 1990. Ionization behavior of native and mutant insulins: p*K* perturbation of B13-Glu in aggregated species. Arch. Biochem. Biophys. 283, 496–502.

Koppel, D.E., 1972. Analysis of macromolecular polydispersity in intensity correlation spectroscopy: the method of cumulants. J. Chem. Phys. 57, 4814–4820.

Kreuter, J., 1988. Nanoparticles. In: Swarbrick, J., Boylan, J.C. (Eds.), Encyclopedia of Pharmaceutical Technology, vol. 10. Marcel Dekker, New York, pp. 165–190.

Lemkine, G.F., Demeneix, B.A., 2001. Polyethylenimines for in vivo gene delivery. Curr. Opin. Mol. Ther. 3, 178–182.

Muller, R.H., 1991. Colloidal Carriers for Controlled Drug Delivery and Targeting. CRC Press, Boston.

Pocker, Y., Biswas, S.B., 1980. Conformational dynamics of insulin in solution. Circular dichroic studies. Biochemistry 19, 5043–5049.

Satake, I., Yang, J.T., 1976. Interaction of sodium decyl sulfate with poly(L-ornithine) and poly-(L-lysine) in aqueous solution. Biopolymers 15, 2263–2275.

Sluzky, V., Tamada, J.A., Klibanov, A.M., Langer, R., 1991. Kinetics of insulin aggregation in aqueous solutions upon agitation in the presence of hydrophobic surfaces. Proc. Natl. Acad. Sci. 88, 9377–9381.

Smith, G.D., Swenson, D.C., Dodson, E.J., Dodson, G.G., Reynolds, C.D., 1984. Structural stability in the 4-zinc human insulin hexamer. Proc. Natl. Acad. Sci. 81, 7093–7097.

Sreerama, N., Venyaminov, S.Y., Woody, R.W., 1999. Estimation of number of α-helical and β-strand segments in proteins using circular dichroism spectroscopy. Protein Sci. 8, 370–380.

Suh, J., Paik, H.-J., Hwang, B.K., 1994. Ionization of poly-(ethyleneimine) and polya(llylamine) at various pH's. Bioorg. Chem. 22, 318–327.

Tiyaboonchai, W., Woiszwillo, J., Middaugh, C.R., 2001. Formulation and characterization of amphotericin B-polyethylenimine–dextran sulfate nanoparticles. J. Pharm. Sci. 90, 902–914.

Tobio, M., Gref, A., Sanchez, A., Langer, R., Alonso, M., 1998. Stealth PLA–PEG nanoparticles as protein carriers for nasal administration. Pharm. Res. 15, 270–275.

Yeo, S.E., Debenedetti, P.G., Patro, S.Y., Przybycien, T.M., 1994. Secondary structure characterization of microparticulate insulin powders. J. Pharm. Sci. 83, 1651–1656.

Zhang, Q., Shen, Z., Nagai, T., 2001. Prolonged hypoglycemic effect of insulin-loaded polybutylcyanoacrylate nanoparticles after pulmonary administration to normal rat. Int. J. Pharm. 218, 75–80.